Journal of Materials Chemistry A

# B/N co-doped carbon nanosphere frameworks as high-performance electrodes for supercapacitors

| | |
|---|---|
| Journal: | *Journal of Materials Chemistry A* |
| Manuscript ID | TA-ART-01-2018-000683.R1 |
| Article Type: | Paper |
| Date Submitted by the Author: | 23-Mar-2018 |
| Complete List of Authors: | Hao, Jian; Jiangsu Normal University, School of Physics and Electronic Engineering<br>Wang, Jiemin; Deakin University, Institute for Frontier Materials<br>Qin, Si; Deakin University, Institute for Frontier Materials<br>Liu, Dan; Deakin University, Institute for Frontier Materials<br>Li, Yinwei; Jiangsu Normal University, School of Physics and Electronic Engineering<br>Lei, Weiwei; Deakin University, Institute for Frontier Materials |
| | |

Journal Name

ARTICLE

# B/N co-doped carbon nanosphere frameworks as high-performance electrodes for supercapacitors

Jian Hao, [†a,b] Jiemin Wang, [†a] Si Qin,[a] Dan Liu,[a]*, Yinwei Li,[b] and Weiwei Lei,[a]*

Received 00th January 20xx,
Accepted 00th January 20xx

DOI: 10.1039/x0xx00000x

www.rsc.org/

Energy storage devices capable of high power outputs currently attract much research interest. An example is supercapacitors, which show both high capacitance and sustained cycling ability. However, their electrodes, especially those based on carbon, often suffer from either low capacitance at high current density or poor durability after many cycles. Here we report a novel boron/nitrogen co-doped carbon nanosphere (B/N-CNS) framework that is simply prepared by annealing boron oxide, ammonium chloride, and glucose. The resulting B/N-CNS exhibits an ultra-high specific capacitance of 423 F $g^{-1}$ at 0.2 A $g^{-1}$ and excellent rate capability of up to 125 F $g^{-1}$ at 50 A $g^{-1}$. The improved performance is ascribed to its interconnected framework of nanospheres and B/N co-doping. In addition, unlike most carbon materials, this framework displays exceptional stability, showing no capacitance fading at 10 A $g^{-1}$ after 30,000 cycles. Furthermore, an all-solid sandwich-structured symmetric supercapacitor with B/N-CNS electrodes can power a light emitting diode, demonstrating its practicability as a fully integrated energy storage device. The facile synthesis strategy and impressive capacitive performances of B/N-CNS framework make this material significantly promising in the fabrication of novel electrode materials for energy storage applications.

## 1. Introduction

To alleviate the serious environmental crisis brought about by over-reliance on fossil fuels for energy, it is vital to rapidly develop new, clean, sustainable, and renewable energy sources.[1] Supercapacitors, a new type of energy-storage device, have attracted considerable research interest because they combine high power density, fast charge/discharge rates, and long cycling stability.[2] Carbon-based nanomaterials have been most widely studied as electrodes in supercapacitors owing to their advantages of lower weight, larger surface area, and better conductivity compared with transition metal oxides and conducting polymers.[3] However, electrodes comprising carbon-based nanomaterials such as graphene and carbon nanotubes tend to provide only electrical double-layer capacitance (EDLC).[3,4] Hence, carbon-based pseudo-capacitive nanomaterials that permit fast reversible redox reactions are highly desirable for improving specific capacitance.[5]

Many studies have suggested doping heteroatoms onto carbon materials as an effective way to enhance pseudo-capacitance, because dopants can modify the electronegativity of carbon atoms to facilitate electro-chemical activity.[6] Boron (B) and nitrogen (N) are suitable candidates due to their small atomic size, strong valence bonding, and similar characteristics to carbon atoms.[7-9] Han *et al.* reported that B-doped graphene nanoplatelets achieved a high specific capacitance of 200 F $g^{-1}$ at 0.1 A $g^{-1}$ in aqueous electrolyte.[10] Similarly, single-N-doped graphene was reported to reach a capacitance of 245.9 F $g^{-1}$ at 1 A $g^{-1}$.[11] More importantly, recent B/N co-doping of carbon materials has delivered higher electro-chemical activity than either B or N single doping owing to synergies in both elements' action.[7-9,12-22] They have also exhibited strong performance in the oxygen reduction reaction (ORR),[23] hydrogen evolution (HER),[24] supercapacitors, and lithium-ion batteries.[12-22,25] Nevertheless, previous B/N co-doped carbon electrodes in supercapacitors have often suffered from either low capacitance at high current density or poor sustained cycling performance, thus impeding further enhancement of energy density and power density as well as limiting their use in integrated energy storage devices. Therefore, it remains a challenge to develop novel B/N co-doped carbon materials with high capacitive performance for practical application.

[a] *Institute for Frontier Materials, Deakin University, Waurn Ponds Campus, Locked Bag 20000, Victoria 3220, Australia.*
[b] *School of Physics and Electronic Engineering, Jiangsu Normal University, Xuzhou, Jiangsu, 221116, China.*
† H. Jian and J. Wang contributed equally to this work.
Electronic Supplementary Information (ESI) available: details of any supplementary information available should be included here. See DOI: 10.1039/x0xx00000x

This work reports the synthesis of B/N co-doped carbon nanosphere (B/N-CNS) frameworks by simply annealing a mixture of boron oxide, ammonium chloride, and glucose. The framework is a dense structure of inter-connected spheres, and has a high surface area (443 $m^2 g^{-1}$). Both B and N are homogeneously doped throughout the whole carbon domain. The produced B/N-CNS framework displays a strong specific capacitance of 423 F $g^{-1}$ at 0.2 A $g^{-1}$ and good rate capability of 125 F $g^{-1}$ at a high current density of 50 A $g^{-1}$. It also shows 106% capacitance retention after 30,000 charge–discharge cycles at 10 A $g^{-1}$, demonstrating its durability to rival the best achieved by any carbon nanomaterials. A B/N-CNS framework symmetric supercapacitor shows both a high energy density of 25 Wh $kg^{-1}$ at a power density of 300 W $kg^{-1}$ and a great power density of 10,550 W $kg^{-1}$ at an energy density of 4.6 Wh $kg^{-1}$. An all-solid integrated symmetric supercapacitor with B/N-CNS framework electrodes demonstrates the material's practicability by powering a light emitting diode (LED). The employed facile synthesis strategy is economical, environmentally friendly, and scalable. The performance of the B/N-CNS framework suggests its suitability as a novel electrode material for energy storage applications.

## 2. Experimental

**Material synthesis:** In a typical synthesis, 0.7g glucose, 6g ammonium chloride and 0.14g boron oxide were mixed in methanol at first. Then the mixture solution was dried to form a white composite under vigorous magnetic stirring. The resultant composite was annealed at 800 °C in a tube furnace for 2 h at a ramp rate of 10 °C $min^{-1}$ in nitrogen flow. After the tube furnace was cooled down to room temperature, a black powder product was collected. For the comparisons, DG800 (only glucose), B-DG800 (glucose and boron oxide) and N-DG800 (glucose and ammonium chloride) were also synthesized under the same condition.

**Material Characterization:** The obtained sample was analyzed with X-ray powder diffraction (XRD, PANalytical X'Pert PRO) with a radiation from a Cu target (K$\alpha$, $\lambda$=0.1541 nm). Fourier transform infrared (FTIR) spectrum was recorded on a Bruker Vertex 70 FTIR in the range of 4000-600 $cm^{-1}$. X-ray photoelectron spectroscopy (XPS) was carried out on an Kratos AXIS Nova instrument equipped with Al Kα X-ray source as the excitation source. Raman spectrum were collected on a Renishaw Raman spectrometer with a laser wavelength of 488 nm at room temperature. Scanning electron microscopy **(**SEM) and X-ray spectroscopy (EDS) mapping were carried out by using a Zeiss Supra 55 VP. Transmission electron microscopy (TEM) was performed on a JEOL 2100F (operating at 200 kV) apparatus. Nitrogen adsorption and desorption isotherms were collected with a Tristar 3000 apparatus at 77 K.

**Electrochemical Test:** The electrochemical measurements were carried out in a three-electrode system with Pt wire as the counter electrode, Ag/AgCl as the reference electrode in 1M $H_2SO_4$ aqueous solution at room temperature. The working electrode consisted of B/N-CNS framework powder, carbon black (Super-P), and polytetrafluoroethylene (PTFE) in a weight ratio of 85:10:5. Ti foil was used as the current collector in acidic medium. CV and GCD tests were conducted using Solartron Analysis electrochemical workstation between -0.2 and 0.7 V (vs Ag/AgCl) at scan rates from 2 to100 mV $s^{-1}$ and the current densities of 0.2-50 A $g^{-1}$, respectively. The gravimetric specific capacitance of the active materials was calculated from constant charge/discharge curves by following equation:

$$C = \frac{I_{cons} t}{m \Delta V} \quad (1)$$

Where $C$ is the gravimetric specific capacitance (F $g^{-1}$), $I_{cons}$ is the constant discharge current (A). $t$ is the discharge time (s), $m$ is the active mass in the electrode (g), and $\Delta V$ is the voltage range.

The cycling stability was studied at 1 A $g^{-1}$, and 10 A $g^{-1}$ within a voltage window of -0.2 to 0.7 V (vs Ag/AgCl).

For two-electrode tests, two pieces of Ti foils with identical sample mass loading were assembled with a cellulose filtering paper as separator. CV studies were conducted within voltage windows of 0–1 V with a scan rate of 5 mV $s^{-1}$. GCD tests were conducted at the current densities of 0.5–20 A $g^{-1}$ between 0–1 V. The energy density E (Wh $kg^{-1}$) and power density P (W $kg^{-1}$) for the Ragone plots were calculated via the following equations based on the total active mass in supercapacitors:

$$E = \frac{CV^2}{2 \times 3.6} \quad (2)$$

$$P = \frac{E}{t} \times 3600 \quad (3)$$

Where V is the voltage after subtracting the ohmic drop (V) and t is the discharge time (h).

For the fabrication of the all-solid sandwich-structured symmetrical B/N-CNS framework supercapacitors, two pieces of B/N-CNS electrodes were sandwiched with PVA-$H_2SO_4$ solid electrolyte, more details could be found in the support information.

## 3. Results and Discussion

In a typical synthesis process, boron oxide, ammonium chloride, and glucose were used as boron, nitrogen, and carbon sources, respectively. The mixture was annealed at 800 °C for 2 h under an $N_2$ flow. The resulting B/N-CNS framework was collected as a black powder after annealing. During pyrolysis, the glucose formed carbon spheres that incorporated both boron and nitride.[26,27] Thermal decomposition of the ammonium chloride released gases that formed pores in the closely packed spheres, thus resulting in a porous interconnected network. Meanwhile, threadlike viscose formed throughout the framework, connecting the nanospheres. They were likely formed by the escaping gas bubbles produced during pyrolysis. Wang *et al.* also reported three-dimensional interconnected struts of graphene derived from glucose and

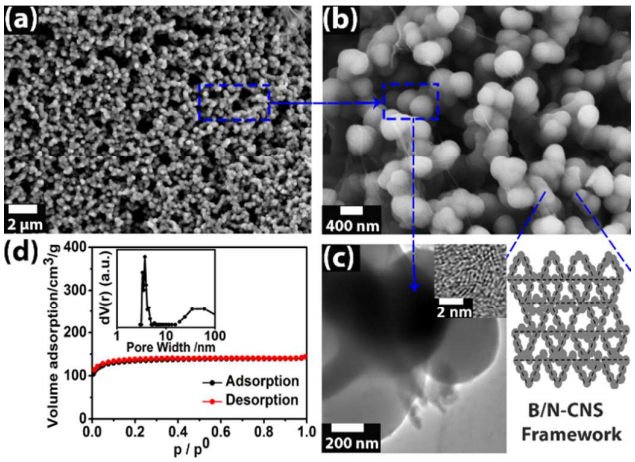


**Fig. 1** Morphology of the B/N-CNS framework. (a) SEM, (b) magnified SEM, and (c) TEM images. The Inset illustrates the HRTEM image and the structure of the framework. (d) Nitrogen adsorption/desorption isotherms. The inset shows the corresponding pore size distribution.

ammonium chloride.[28] The morphology of B/N-CNS is shown in **Fig. 1**. Scanning electron microscopy (SEM) images depict the framework as interlaced nanosphere clusters (Fig. 1a). The surfaces of the nanospheres are competely smooth with a layer of sticky viscos wrapping (Fig. 1b). The nanospheres have an average diameter of around 500 nm, as shown in Fig. 1b and the transmission electron microscopy (TEM) image (Fig. 1c). Compared with carbon spheres synthesized by the hydrothermal treatment of glucose,[26,27] these particles are smaller and more homogenous. The closely packed, uniformly dispersed nanospheres are connected by sticky threadlike viscos, forming a porous cobweb framework (Fig. 1a, inset of 1c and Fig. S1). In addition, high-resolution TEM (HRTEM) (inset of Fig. 1c and Fig. S1b) reveals 3–8 parallel fringes on the nanospheres with both crystalline and amorphous-like phases. The interlayer distance is calculated to be 0.37 nm, similar with previously reported BCN nanomaterials.[9,23] The dense interconnected framework possibly benefits the capacitance and cycling stability of B/N-CNS in the electrolyte. The nitrogen adsorption–desorption isotherm is shown in Fig.1d.[23] The Brunauer–Emmett–Teller (BET) specific surface area is 504 $m^2 g^{-1}$, with a total pore volume of 0.7 $m^3 g^{-1}$, which is larger than that for most reported carbon nanospheres.[29,30] The large surface area and pore volume further contribute to the electrochemical activity of the framework.

**Figure 2** shows the chemical composition of the B/N-CNS framework. The powder X-ray diffraction (XRD) pattern in Fig. 2a shows two broad characteristic humps at around 25° and 43°, respectively, representing the (002) and (101) planes of the framework, similar with Other B/N co-doped carbon nanomaterials.[9,25] The Fourier transform infrared (FTIR) spectrum (Fig. 2b) has two bands at around 1380 and 800 $cm^{-1}$ that are attributable to B–N stretching and bending, respectively.[23] The Raman spectrum shows D- (1355 $cm^{-1}$) and G- (1593 $cm^{-1}$) bands as well as two weak 2D and D+G bands (at 2700 and 2900 $cm^{-1}$) (Fig. 2c), consistent with previously reported B/N co-doped carbon nanomaterials.[24] The $I_D/I_G$ intensity ratio is 0.972, suggesting the existence of defects generated by heteroatoms doping in the graphitic carbon network.[17] X-ray photoelectron spectroscopy (XPS) was further used to investigate the chemical composition in B/N- CNS. The atomic ratio is $B_1N_{1.81}C_{10.98}O_{2.23}$ (i.e., 6.24, 11.30, 68.51 and

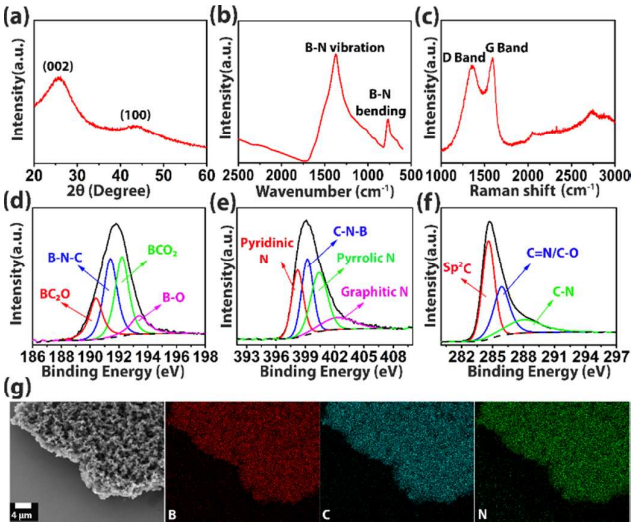


**Fig. 2** Characterization of the B/N-CNS framework: (a) XRD pattern, (b) FTIR spectrum, (c) Raman spectrum, (d) XPS B 1s spectrum, (e) XPS N 1s spectrum, (f) XPS C 1s spectrum, and (g) SEM image and corresponding EDS mapping images of B, C, and N elements.

13.94 at.% respectively; Fig. S2a). The B 1s signal could be deconvoluted into four peaks centered at 190.38, 191.38, 192.18, and 193.40 eV, corresponding to $BC_2O$, B–N–C, $BCO_2$, and B–O bonds, respectively (Fig. 2d).[19,22] Previous studies have shown that attached groups containing B could improve the specific capacitance of carbon materials.[10,22] The N1s spectrum in Fig. 2e was fitted to four peaks: pyridinic N (~398.17 eV), C–N–B (~399.21 eV), pyrrolic N (~400.37 eV), and quaternary N (~402 eV).[23] Notably, the dominant pyridinic and pyrrolic N (58.07% in the N 1s area) could also help enhance the capacitance by introducing pseudo-capacitance through faradic redox reactions.[11,22] The C 1s signal in Fig. 2f consists of three peaks centered at 284.46 ($sp^2$ C), 285.55 (C=N/C–O), and 287.75 eV (C–N).[16,17] Moreover, from the O 1s spectrum in Fig.S2b, it could be seen there are C-O/C=O and B-O bonds in the samples, which may improve the wettability (hydrophilicity) between electrolyte and electrode materials.[23] Energy-dispersive X-ray spectrometry (EDS) mapping (Fig. 2g) confirms the homogeneous distributions of B, C, and N in the B/N-CNS framework. The above XRD, FTIR, Raman, XPS, and EDS mapping results clearly show the doping of both B and N atoms into the C nanospheres. The incorporation of heteroatoms promoted the electrochemical performance of the B/N-CNS framework.

The electrochemical performance of the B/N-CNS framework as an electrode in a three-electrode supercapacitor was investigated in 1 M $H_2SO_4$. **Fig. 3**a shows cyclic voltammetry (CV) curves for the framework at scan rates from 2 to 100 mV $s^{-1}$. Unlike the EDLC of carbon materials such as graphene, the curve is quasi-rectangular with a pair of redox peaks at around −0.2 V (vs Ag/AgCl), demonstrating reversible faradaic pseudocapacitance due to B/N heteroatom electrochemical polarization.[4,17] Moreover, this distinctive shape remains unchanged as the scan rate increases from 2 to 100 mV $s^{-1}$, confirming the fast kinetics for electrical double layer formation and faradic reactions over the B/N-CNS framework.[13] Galvanostatic charge–discharge (GCD) profiles are

shown in Fig. 3b; The B/N-CNS framework delivers an impressive ultra-high capacitance of 423 F $g^{-1}$ at a current density of 0.2 A $g^{-1}$, which is

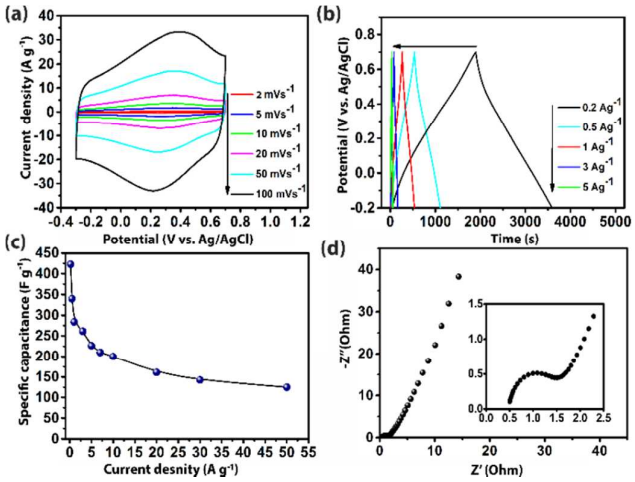


**Fig. 3** Electrochemical performances of B/N-CNS framework electrodes in 1 M $H_2SO_4$ electrolyte. (a) CV curves at scan rates of 2–100 mV $s^{-1}$. (b) GCD curves at current densities of 0.2–5.0 A $g^{-1}$. (c) Specific capacitance at various current densities. (d) Nyquist plot of electrochemical impedance at 100 kHz to 10 mHz. The inset shows the characteristic high-frequency semicircle shape.

higher than that of most recently reported B/N doped carbon materials (Table S1).[12-22] High capacitance could also be maintained over a wide range of current densities from 0.2 to 50 A $g^{-1}$ (Fig. 3c). Normally, most carbon-based materials degrade rapidly under high current charge/discharge (above 10 A $g^{-1}$) and deactivate. [14,16,18] The B/N-CNS framework, in contrast, had a specific capacitance of 125 F $g^{-1}$ even at a large current density of 50 A $g^{-1}$. The improved conductivity shown by the supercapacitor is likely due to the enhanced surface-to-volume ratio of the nanospheres, the interconnected structure, and the topological configuration of the framework jointly reducing the transport lengths for both ion and electron transfer.[28,29] This is further supported by the electrochemical impedance spectroscopy (EIS) results in Fig. 3d. The near-vertical low-frequency region of the Nyquist plot indicates fast ion diffusion and migration in the electrode.[19] The high-frequency semicircle with small diameter reflects low internal charge-transfer resistance during faradic reactions.[15] Therefore, the light doping of B and N in these carbon spheres not only enables pseudocapacitance, but also improves the ion diffusion (Fig. S5), which are beneficial to the charging–discharging process at high current density. The cycling stability of the B/N-CNS framework was tested under 10 A $g^{-1}$ as shown in **Fig. 4**. At a relatively low charge–discharging current density of 1 A $g^{-1}$, 100% of the specific capacitance retained after 5000 cycles (Fig. S6). However, increasing the current density to 10 A $g^{-1}$ gradually increased the capacitance retention to 106% after 30,000 cycles (Fig. 4a). This is further demonstrated by GCD (Fig. 4a inset) and CV (Fig. 4b) curves before and after sustained cycling at 10 A $g^{-1}$ (Fig. 4b). The promotion of capacitance after cycling at high current density is attributed to B,N-induced electro-activation, improved wettability of the electrodes during fast charging and discharging, and accessibility of the pores to the electrolyte.[16,19] The sticky porous nanospheres enhanced the stability of the framework, resulting in improved cycling durability. The faradaic pseudocapacitance peaks in the CV curve gradually expanded and became intense within initial 10,000 cycles, especially during sustained charging–discharging cycling at 10 A $g^{-1}$; they remained stable between 10,000 and 30,000 cycles (Fig. S7). This was due to the B, N dopants improving faradaic pseudo-capacitance during cycling. The closely packed and well-connected nanospheres stabilized the structure and provided an excellent electron and ion percolation network during cycling. Fig. 4c and d compares the performances of various B/N-doped carbon materials as supercapacitor electrodes. To our knowledge, the B/N-CNS framework exhibits the highest specific capacitance (423 F $g^{-1}$ at 0.2 A $g^{-1}$) (Fig. 4c) and greatest sustained cycle retention (106% after 30,000 cycles at 10 A $g^{-1}$) (Fig. 4d) of any reported B/N-doped carbon material or hybrid (**Table S1**). Overall, appropriate B/N co-doping and a suitable nanosphere architecture with high surface area result in high capacitance and extended stability that is potentially useful for industrial supercapacitors.

The capacitive performance of a symmetrical B/N-CNS framework supercapacitor is tested in a two-electrode configuration in 1 M $H_2SO_4$. **Fig. 5**a shows GCD plots at various current densities in the potential window of 0 to 1 V. The anodic charging and corresponding cathodic discharging curves are generally symmetric, indicating a high degree of reversibility, and is consistent with the symmetric quasi-rectangular CV curves (Fig. S8). The calculated capacitance is 60 F $g^{-1}$ at 0.5 A $g^{-1}$ and 24 F $g^{-1}$ at 20 A $g^{-1}$, with the corresponding voltage (IR) drop increasing (Fig. 5b). The values are smaller than those of a three-electrode system. For the reason that, the capacitance of the symmetrical device based on the full cell including two-electrodes is theoretically 1/4 of the value of a single electrode.[20] In addition, in this two-electrode configuration, Ti foil

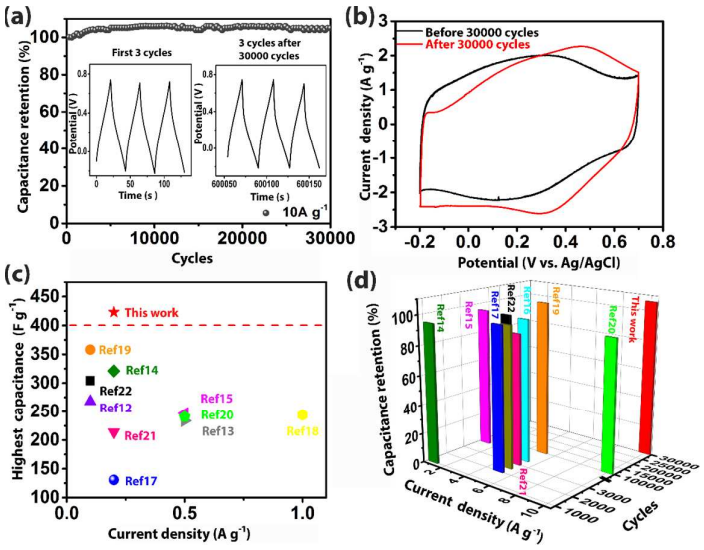


**Fig. 4** Cycling stability of a B/N-CNS framework electrode in 1 M $H_2SO_4$ electrolyte. (a) Capacitance retention during 30,000 cycles at

10 A $g^{-1}$; inset shows GCD curves before and after cycling. (b) CV curves before and after similar cycling obtained at a scan rate of 5 mV $s^{-1}$. Comparison of (c) specific capacitance and (d) capacitance retention with results reported for other B/N-doped carbon electrodes.

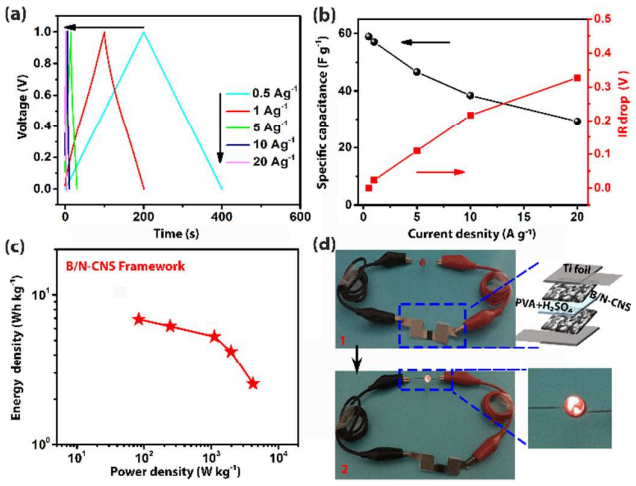


**Fig. 5** Capacitive performance of a symmetrical B/N-CNS framework supercapacitor. (a) GCD curves at current densities of 0.5–20 A $g^{-1}$. (b) Specific capacitance and IR drop potential at various current densities. (c) Ragone plot of the B/N-CNS framework. (d) Photographs of an LED powered using two tandem all-solid sandwich-structured symmetrical B/N-CNS framework supercapacitors. (1. Before LED charging; 2. during charging).

and cellulose filtering paper were used as current collector and separator, respectively, which may increase the impedance and reduce the ion diffusions as well. Moreover, the decreased capacitance is also related to the high mass loading of the electrodes employed.[19] There is no obvious IR drop at small current densities (0.5 and 1 A $g^{-1}$), indicating low internal resistance. Even the increased IR drop at large current density is still reasonable compared with results for other B/N-doped carbon materials[5,19,31] due to the intrinsic resistance properties of those carbon materials. The energy density and power density for various materials are given in the Ragone plot in Fig. 5c. An energy density (E) of 6.9 Wh $kg^{-1}$ was achieved here, based on the GCD curve at 0.5 A $g^{-1}$, with a corresponding power density (P) of 80 W $kg^{-1}$. In addition, the maximum gravimetric power density was 2700 W $kg^{-1}$ (E = 2.1 Wh $kg^{-1}$) at 20 A $g^{-1}$. These values are comparable to other reported B/N-doped carbon materials.[19,20] To evaluate the practicability of this material as a supercapacitor, an all-solid sandwich-structured symmetrical B/N-CNS framework supercapacitor cell was fabricated (Fig. S9). It was both lightweight (200 mg) and thin (0.57 mm), thus easily portable. More importantly, the mass loading of each electrode of a single cell was only around 1 mg, and two series-wound cells lit a LED bulb (Fig. 5d). The relatively low mass loading and efficient power ability suggest that

this integrated portable supercapacitor device based on the B/N-CNS framework is applicable to large-scale manufacturing.

## Conclusions

In conclusion, a novel boron/nitrogen co-doped carbon nanospheres (B/N-CNS) framework has been successfully synthesized by a facile yet scalable route. The as-obtained sample constitutes of a cobweb interconnected nanospheres framework with a high BET surface area of 443 $m^2$ $g^{-1}$. More significantly, as supercapacitor electrodes, the B/N-CNS framework delivers an ultra-high capacitance of 423 F $g^{-1}$ at 0.2 A $g^{-1}$ and achieves super long-life stability with 106% retention within 30000 cycles at 10 A $g^{-1}$ charging/discharging. The B, N co-doping effect, unique nanosphere framework and rational porosity enable the remarkable electrochemical properties. In addition, this material with both comparable power density and energy density is promising in the application of integrated portable supercapacitors. Hence, this study provides an effective strategy to construct novel B, N co-doped carbon nanomaterials with extra-high capacitive performances, which could satisfy the greater demand of practical energy storage devices.

## Acknowledgements

This work was financially supported by the Australian Research Council Discovery Early Career Researcher Award scheme (DE150101617 and DE140100716), Deakin University, Central Research Grant Scheme, the National Natural Science Foundation of China under Grant Nos. 11722433 and 11404148.

## Notes and references

1 B. M. Sánchez, Y. Gogotsi, *Adv. Mater.* 2016, **28**, 6104.
2 G. Wang, L. Zhang, J. Zhang, *Chem. Soc. Rev.* 2012, **41**, 797.
3 L. Zhang, X. S. Zhao, *Chem. Soc. Rev.* 2009, **38**, 2520.
4 M. D. Stoller, S. Park, Y. Zhu, J. An, R. S. Ruoff, *Nano Lett.*, 2008, **8**, 3498.
5 Z. Wu, A. Winter, L. Chen, Y. Sun, A. Turchanin, X. Feng, K. Müllen, *Adv. Mater.* 2012, **24**, 5130.
6 Z. Zhao, M. Li, L. Zhang, L. Dai, Z. Xia, *Adv. Mater.* 2015, **27**, 6834.
7 J. Wu, M. F. Rodrigues, R. Vajtai, P. M. Ajayan, *Adv. Mater.*2015, **26**, 6239.
8 N. kumar, K. Moses, K. Pramoda, S. N. Shirodkar, A. K. Mishra, U. V. Waghmare, A. Sundaresan, C. N. R. Rao, *J. Mater. Chem. A* 2013, **1**, 5806.
9 J. Wang, J. Hao, D. Liu, S. Qin, C. Chen, C. Yang, Y. Liu, T. Yang, Y. Fan, Y. Chen, W. Lei, *Nanoscale* 2017, 9, 9787.
10 J. Han, L. Zhang, S. Lee, J. Oh, K. Lee, J. R. Potts, J. Ji, X. Zhao, R. S. Ruoff, S. Park, *ACS Nano* 2013,**7**,19.
11 Z. Wen, X. Wang, S. Mao, Z. Bo, H. Kim, S. Cui, G. Lu, X. Feng, J. Chen, *Adv. Mater.* 2012, **24**, 5610.
12 H. Guo, Q. Gao, *J. Power Sources* 2009, **186**, 551.
13 H. Konno, T. Ito, M. Ushiro, K. Fushimi, K. Azumi, *J. Power Sources* 2010, **195**, 1739.
14 E. Iyyamperumal, S. Wang, L. Dai, *ACS Nano* 2012, **6**, 5259.
15 D. Guo, J. Mi, G. Hao, W. Dong, G. Xiong, W. Li, A. Lu, *Energy Environ. Sci.* 2013, **6**, 652.
16 J. Zhou, N. Li, F. Gao, Y. Zhao, L. Hou, Z. Xu, *Sci. Rep.* 2014, **4**, 6083.

17 S. Dou, X. Huang, Z. Ma, J. Wu, S. Wang, *Nanotechnology* 2015, **26**, 045402.
18 I. Karbhal, R. R. Devarapalli, J. Debgupta, V. K. Pillai, P. M. Ajayan, M. V. Shelke, *Chem. Eur. J.* 2016, **22**, 7134.
19 Z. Ling, Z. Wang, M. Zhang, C. Yu, G. Wang, Y. Dong, S. Liu, Y. Wang, J. Qiu, *Adv. Funct. Mater.* 2016, **26**, 111.
20 Q. Hao, X. Xia, W. Lei, W. Wang, J. Qiu, *Carbon* 2015, **81**, 552.
21 B. You, F. Kang, P. Yin, Q. Zhang, *Carbon* 2016, **103**, 9.
22 H. Chen, Y. Xiong, T. Yu, P. Zhu, X. Yan, Z. Wang, S. Guan, *Carbon* 2017, **113**, 266.
23 J. Wang, J. Hao, D. Liu, S. Qin, D. Portehault, Y. Lin, Y. Chen, W. Lei, *ACS Energy Lett.* 2017, **2**, 306.
24 M. Chhetri, S. Maitra, H. Chakraborty, U. V. Waghmare, C. N. R. Rao, *Energy Environ. Sci.* 2016, **9**, 95.
25 W. Lei, S. Qin, D. Liu, D. Portehault, Z. Liu, Y. Chen, *Chem commun.* 2013, **49**, 352.
26 Y. Mi, W. Hu, Y. Dan, Y. Liu, *Mater.Lett.* 2008, **62**, 1194.
27 M. Li, W. Li, S. Liu, *Carbohydr. Res.* 2011, **346**, 999.
28 X. Wang, Y. Zhang, C. Zhi, X. Wang, D. Tang, Y. Xu, Q. Weng, X. Jiang, M. Mitome, D. Golberg, Y. Bando, *Nature Commun.* 2013, **4**, 2905.
29 H. Wang, L. Shi, T. Yan, J. Zhang, Q. Zhong, D. Zhang, *J. Mater. Chem. A* 2014, **2**, 4739.
30 J. Tang, J. Liu, C. Li, Y. Li, M. O. Tade, S. Dai, Y. Yamauchi, *Angew. Chem. Int. Ed.* 2015, **54**, 588.

## The table of contents entry:

**A** novel B/N co-doped carbon nanospheres framework is synthesized by a facile, economic, environmental and scalable method. The as-obtained materials display extra-high capacitive performance and exceptional long cycle stability with the merits of high energy and power density. We believe that this material will be applicable in the application of integrated energy storage devices.